33RD INTERNATIONAL COSMIC RAY CONFERENCE, RIO DE JANEIRO 2013
THE ASTROPARTICLE PHYSICS CONFERENCE

Precision measurement of the $e^+ + e^-$ spectrum with AMS

B.BERTUCCI[1], ON BEHALF OF THE AMS-COLLABORATION[2].

[1] *Università degli Studi di Perugia and INFN sezione di Perugia*
[2] *For the complete list of the authors see the AMS Collaboration list, these proceedings.*

Bruna.Bertucci@pg.infn.it

Abstract: The AMS-02 detector is operating on the International Space Station since May 2011. More than 30 billion events have been collected by the instrument in the first two years of data taking, among them $\sim$ 9 million of electrons and positrons have been selected to measure the combined electron plus positron energy spectrum in the energy range from 0.5 to 700 GeV. In this contribution, we will review the analysis techniques used in the combined electron plus positron energy spectrum measurement.

Keywords: cosmic rays, ISS, electrons, AMS.

1 Introduction

Cosmic Ray Electrons [1] (CRE) represent only a small fraction of the Cosmic Rays reaching the earth's atmosphere. Nevertheless the relevance of their flux and charge composition is fully recognized and has triggered a continuous experimental effort during the last 50 years.
Due to their small masses, the energy losses experienced by the CRE during their propagation in the Galaxy are fundamentally different with respect to those of the nuclear components and the features of the CRE energy spectrum above $\sim$ 10 GeV are sensitive to their production in nearby sources [1]. An excess of electrons in the range 300-700 GeV with respect to the expected spectrum from conventional diffuse electron sources has been reported by ATIC [2] and PPB-BETS [3]. The following measurements of FERMI [4, 5] observed a spectral flattening of the CRE spectrum between 70-200 GeV and a milder excess at higher energies with respect ATIC and PPB-BETS. At higher energies, a rapid steepening of the spectrum is observed by HESS [7, 6]. The PAMELA measurements of the positron fraction [8] and the e^- spectrum [9] have pointed to the need of a *fresh* source of electrons and positrons contributing to the observed features in the high energy part of the CRE spectrum. The accurate AMS-02 measurement of the positron fraction at energies up 350 GeV [10] is well described by assuming for each species a spectrum composed by the sum of a power law, with different spectral indexes for e^- and e^+, and a common source term with a cutoff energy dominating the higher energy part of their spectra. Accurate measurements of the features of the CRE up to TeV energies can shed light on the origin of these observed features, either from exotic sources such as dark matter particles or other astrophysical sources such as pulsars [12].

The large statistics collected in two years of the AMS-02 mission on board of the ISS has been analysed to perform accurate measurements of the CRE spectrum, the individual e^+ and e^- fluxes and the positron fraction in the CRE flux. Independent analyses with different sources of systematic uncertainties have been used for the different measurements and are presented at this conference [13, 14]. In this contribution, we will review the analysis techniques used in the CRE spectrum measurement.

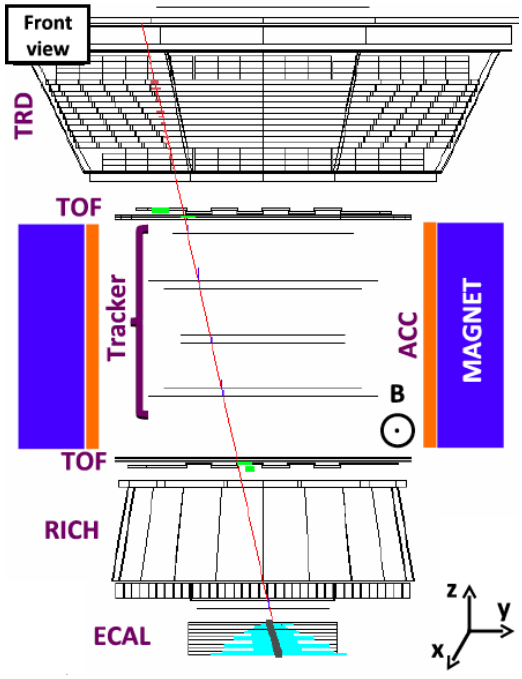

Figure 1: AMS-02 detector schematics in the event display of a 600 GeV electron.

2 The AMS-02 Detector

The layout of the AMS-02 detector [10] is shown in Fig.1 presenting the event display of a 600 GeV electron recorded by AMS. It consists of nine planes of precision silicon tracker, a transition radiation detector (TRD), four planes of time of flight counters (TOF), a permanent magnet, an array of anticoincidence counters (ACC) surrounding the inner tracker, a ring imaging Cerenkov detector (RICH), and an electromagnetic calorimeter (ECAL).
The TRD is designed to use transition radiation to distinguish between electrons and protons, and *dE/dx* to independently identify nuclei. It consists of 5248 proportional tubes of 6 mm diameter with a maximum length of 2 m

1. Whenever not explicitly distinguished in the text we will refer to Cosmic Ray Electrons as including also the positron component

arranged side by side in 16-tube modules. The 328 modules are mounted in 20 layers. Each layer is interleaved with a 20 mm thick fiber fleece radiator (LRP375) with a density of 0.06 g/cm^3. There are 12 layers of proportional tubes along the y axis located in the middle of the TRD and, along the x axis, four layers located on top and four on the bottom. The tubes are filled with a 90:10 Xe:CO2 mixture. In order to differentiate between electron and protons, signals from all the TRD layers are combined in a log-likelihood probability of the electron (TRD-LLe) or proton (TRD-LLp) hypothesis. The ratio of these probabilities has been used in the AMS-02 positron fraction as e/p discriminator. Two planes of TOF counters are located above and two planes below the magnet. Each plane contains eight or ten scintillating paddles. Each paddle is equipped with two or three photomultiplier tubes on each end for efficient detection of traversing particles. The average time resolution of each counter has been measured to be 160 ps, and the overall velocity ($\beta = v/c$) resolution of the system has been measured to be 4% for $\beta \simeq 1$ Z=1 particles which also discriminates between downward and upward-going particles. The coincidence of signals from all four TOF planes provides the charged particle trigger.
The ECAL consists of a multilayer sandwich of lead and scintillating fibers with an active area of 648×648 mm^2 and a thickness of 166.5 mm corresponding to 17 radiation lengths The calorimeter is composed of nine superlayers, each 18.5 mm thick. In each superlayer, the fibers run in one direction only. The 3D imaging capability of the detector is obtained by stacking alternate superlayers with fibers parallel to the x and y axes (five and four superlayers, respectively). The fibers are read out on one end by 1296 photosensors with a linearity of $1/10^5$ per sensor. Signals from three super layers in y view (super layers 2,4,6) and in x view (super layers 1,3,5) are used in the trigger logic to select events with a shower in the calorimeter.

In the electron measurement, the TOF detector is used to select Z=1 relativistic particles traversing the AMS-02 in the downward direction with respect the AMS-02 reference system. The different characteristics of the signal released by protons, nuclei and electrons in the TRD and ECAL detectors are used to identify the electron component. A track reconstructed at least in the inner tracker (planes 2 to 8) and matching the TRD and ECAL signals is used to select clean Z=1 events in the apparatus. Specific calibration procedures of all sub-detectors have been developed in order to guarantee the stability of the AMS-02 performances over time and no significant degradation of the apparatus has been observed during two years of operation in space. Details on the sub-detector performances and calibration procedures are also presented in this conference [15, 16, 17, 18].

3 The data analysis

The main challenge of the analysis is to identify and efficiently select electrons within the overwhelming background of protons and helium nuclei in a wide energy range. The TRD and ECAL detectors are the key instruments used to achieve this difficult task.
A loose preselection is first applied to the collected events in order to keep only down going relativistic particles ($\beta > 0.8$) with associated signals in the TRD and in the ECAL. In order to reject particles produced by the interaction of primary cosmic rays with the atmosphere, the energy

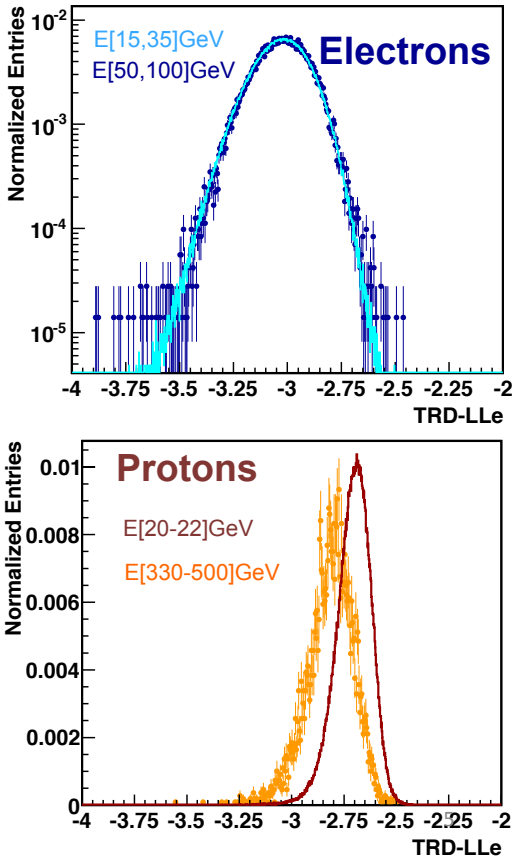

Figure 2: TRD-LLe distribution for electrons (top) and protons (bottom) in different energy ranges.

measured with the ECAL is required to exceed by a factor of 1.25 the maximal Stoermer cutoff for either a positive or a negative particle at the geomagnetic location where the particle was detected and at any angle within the AMS acceptance. This set of requirements constitutes the event preselection and is used in the time exposure and acceptance definitions as discussed in Sec.4.
Z>1 particles are rejected by means of the signal released in the TRD and the Tracker.

3.1 Selection and measurement technique

The electron measurement is performed in ECAL energy bins. The binning is chosen according to the energy resolution and the available statistics such that migration of the signal events to neighbouring bins has a negligible contribution to the systematic errors above 2 GeV. In each energy bin, the reference spectra of the TRD-LLe estimator for electrons and protons is fitted to data varying the normalisations of the signal and the background components.
The reference spectra for signal and background are evaluated directly from the flight data. For this purpose, pure samples of electrons and protons are selected by means of tight requirements on the ECAL shower shape, the comparison between reconstructed momentum in the Tracker and measured energy in the ECAL, as well as the reconstructed charge sign. Figure 2 shows the distribution of the TRD-LLe estimator for electrons (top) and protons (bottom) in different energy ranges. As expected, the TRD-LLe distribution shows no dependence on the electron energy above $\sim$ 10 GeV. Thus a unique template function is defined from

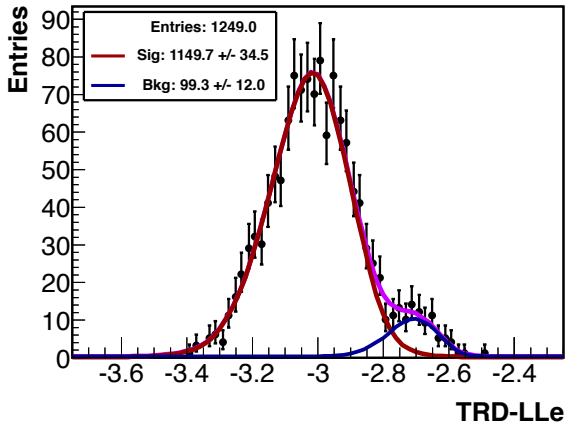

Figure 3: TRD likelihood estimator distribution in the energy range 102.5-109.4 GeV. Signal and background components are represented by the red and blue curves respectively. The magenta line represents the overall fit superimposed on the black data points.

all electrons selected in the 10-100 energy range and it is used to represent the signal shape up to the highest energies. To define the proton template at lower electron energies, the TRD-LLe reference distributions are evaluated separately in each energy interval.
The fitting procedure is repeated applying different calorimetric selection of the events. A statistical estimator, based on a Boosted Decision Tree algorithm (BDT), is used to fully exploit the 3D shower reconstruction capability of the ECAL. Different cuts on the ECAL BDT estimator are applied to vary the electron purity of the samples and the BDT cut applied in the analysis is chosen such as to minimise the combined systematics and statistical uncertainties. In Fig. 3 an example of the fitted signal and background distributions are presented at energies between 102.5 and 109.4 GeV.

4 The flux measurement

The electron flux in each energy interval [E,E+Δ E] is measured as :

$$\Phi(E,E+\Delta E) = \frac{N(E)}{\Delta E A(E) \Delta T(E) \varepsilon(E)}$$

where:

- N is the number of electron events;
- ΔT is the exposure time, 51.6×10^6 s at energies above 25 GeV;
- A is the the effective detector acceptance after applying the event selection;
- ε is the combined efficiency of the trigger and signal selection;

A full MonteCarlo simulation of the response of the AMS-02 detector to an isotropic electron spectrum is used to calculate the detector acceptance.
Given the Geometric Factor (GF) of the surface used to generate the events, the acceptance is defined as:

$$A(E,E+\Delta E) = GF \times \frac{N_{acc}}{N_{gen}}$$

where N_{acc} and N_{gen} represent respectively the number of selected and generated events in the energy interval [E,E+ΔE]. The efficiency of each selection cut is evaluated on data and compared to the expectations from simulation. As assessment of the systematic uncertainties on the acceptance and selection efficiencies are still ongoing, some examples of the examined quantities will be presented.

4.1 Trigger efficiency

Different trigger conditions are implemented in the AMS-02 trigger logic to maximize the efficiency for different particle species while keeping a sustainable rate of the recorded events. Electron events are acquired by either one of the three following conditions:
- *single charge trigger* : the coincidence of signals from all the four TOF planes is required in anti coincidence with the ACC ;
- *electron trigger*: as for the single charge trigger the four TOF planes coincidence is required, no veto is applied from the ACC signal if energy deposits above threshold are measured in at least two out out of the three ECAL superlayers used in the trigger in both the x and y views;
- *photon trigger*: no coincidence of signals from the four TOF planes is found, but there is a shower pointing within the AMS acceptance. A fast reconstruction algorithm is used at the level of the trigger logic to evaluate the shower direction from the signals over threshold registered in the x and ECAL super layers views used in the trigger.

In order to measure the trigger efficiency from data, a pre scaled sample of events passing looser trigger conditions is also recorded as an *unbiased* sample. In particular, 1/100 of the events with a coincidence of signals from at least 3 TOF planes are recorded, irrespectively of any veto from the ACC, and 1/1000 of the events having an energy deposit in the ECAL satisfying the electron trigger condition.
The trigger efficiency is then evaluated from the fraction of electrons selected by the trigger over the total number of electrons in the triggered + *unbiased* sample, taking into account the appropriate prescaling factor. In Fig.4 the trigger efficiency as a function of energy is presented. Above a few GeVs, no unbiased events were present in the electron sample and the measured efficiency is 100%. At lower energies, as the energy deposit in the calorimeter decreases, the requirement of the electromagnetic trigger becomes too tight and a reduction of the trigger efficiency is observed due to the effect of the ACC veto.

4.2 Track reconstruction efficiency

The efficiency of having a reconstructed track associated to an electron passing through the tracker acceptance has been

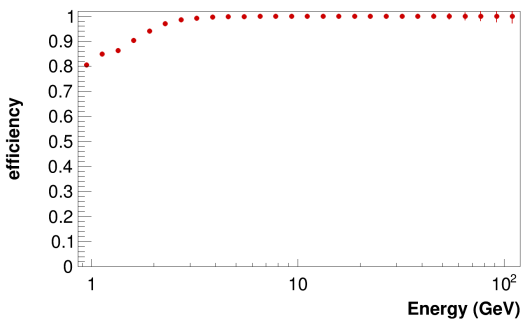

Figure 4: Trigger efficiency as a function of energy

studied in data as a function of energy. For this estimate, the same requirements used in the electron analysis flow are applied to the data sample, except the requirement of a track. The efficiency has been defined from the ratio of the number of electrons with an associated track over the total number of electrons, both quantities are evaluated for particles passing through the geometrical acceptance of the tracker. In Fig.5 the tracker efficiency as a function of the energy is shown. Data and MonteCarlo estimates are in agreement at the one % level over a wide energy range.

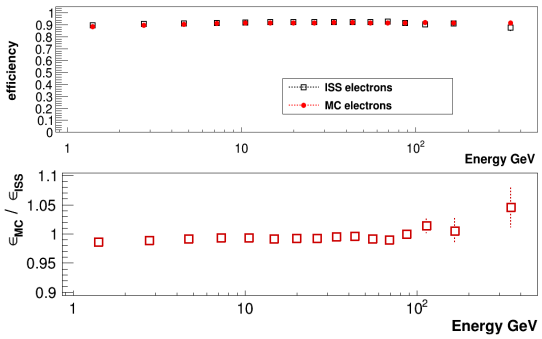

Figure 5: Track reconstruction efficiency as a function of energy

4.3 ECAL BDT selection efficiency

In each energy interval the measurement is performed at the ECAL BDT cut that minimizes the overall measurement uncertainties. The ECAL BDT efficiency is evaluated from a probe sample of electrons, chosen with tight requirements on the energy/momentum ratio and a negative charge sign. The template fit analysis is performed on this sample at different BDT cuts and the ratio between fitted electrons at a given BDT cut vs the total number of fitted electrons in absence of calorimetric selection defines the efficiency. The stability of the measurement against different selection efficiencies is shown in Fig.6 where the number of electrons corrected by the BDT efficiency is shown as a function of different efficiencies in the BDT cut applied before performing the template fit analysis. The RMS of the distribution is $<1\%$ over a wide range leading to a minor contribution to the overall measurement uncertainty.

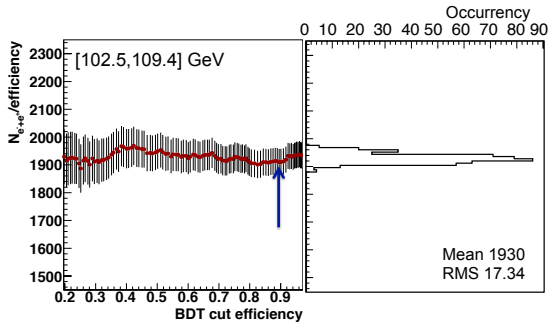

Figure 6: Stability of the measured number of electrons as a function of the ECAL BDT cut efficiency. The blue arrow indicates the working point in the presented measurement.

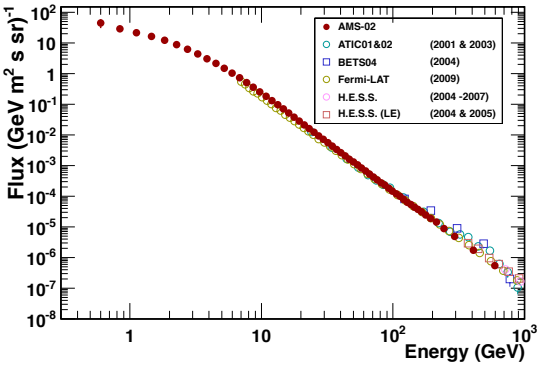

Figure 7: AMS combined electrons+positron spectrum (red points) superimposed to recent measurements from references [2, 3, 4, 6, 7]

5 Conclusions

The measurement of the electron spectrum with the AMS-02 detector has been performed at energies between 0.5 and 700 GeV and is reported in Fig.7. The assessment of systematic uncertainties is currently being finalised. For this measurement, $\sim$ 9 million electrons have been selected from more than 30 billion trigger collected in two years of operation in space. This represents $\sim$ 10% of the expected AMS data sample.

From this preliminary study, no evidence has been found of structures in the electrons energy spectrum such as those observed by ATIC and PPB-BETS. However, a change in the spectral distribution with increasing electron energies can be seen, which is better appreciated in the separate measurements of the e^- and e^+ components of the flux [14]. In the current understanding of the measurement uncertainties, this change could be compatible with the phenomenological description of the electron and positron components observed in the AMS-02 positron fraction measurement.

Acknowledgment: This work has been supported by acknowledged person and institutions in [10] as well as by the Italian Space Agency (ASI) under contract ASI-INFN I/002/13/0 and ASDC/011/11/1

References

[1] T.Delahaye *et al*, Astron. & Astroph. 524 (2010) A51
[2] J.Chang *et al*, Nature 456 (2008) 362 -365
[3] S.Torii *et al*, ArXiv:0809.0760
[4] M.Ackerman *et al*, Phys. Rev. D 82 (2010) 092004
[5] M.Ackerman *et al*, Phys. Rev. Lett. 108 (2012) 011103
[6] F.Aharonian *et al*, Phys. Rev. Lett. 101 (2008) 261104
[7] F.Aharonian *et al*, A&A 508 (2009) 561- 564
[8] O.Adriani *et al*, Nature 458 (2009) 607-609
[9] O.Adriani *et al*, Phys. Rev. Lett. 106 (2011) 201101
[10] M.Aguilar *et al*, Phys. Rev. Lett. 110 (2013) 141102
[11] T.Delahaye *et al*, Astron. & Astroph. 501 (2009) 821-833
[12] Phys. Rev. Lett 103 (2010) 051104
[13] A.Kounine, this conference [ID 1246]
[14] S.Schael, this conference [ID 1257]
[15] C.Delgado *et al*, this conference [ID 1260] , J.Bazo *et al*, this conference [ID 0849] , P.Zuccon *et al*, this conference [ID 1064]
[16] H.Gast *et al*, this conference [ID 0359]
[17] Q.Yan *et al*,this conference [ID 1097]
[18] Di Falco *et al*, this conference [ID 0855]